Epitaxial silicon minority carrier diffusion length by photoluminescence

D. H. Baek,[1,a)] S. B. Kim,[2] and D. K. Schroder[1]
[1]*Department of Electrical Engineering, Arizona State University, Tempe, Arizona 85287-5706, USA*
[2]*SUMCO Phoenix Corporation, Arizona 85050, USA*

(Received 5 June 2008; accepted 9 July 2008; published online 3 September 2008)

Photoluminescence (PL) is a convenient contactless method to characterize semiconductors. Its use for room-temperature silicon characterization has only recently been implemented. We have developed the relevant theory and compared it with experimental data initially for bulk Si wafers and then extended it to moderately doped epitaxial layers on heavily doped substrates. Our theory predicts the PL behavior as a function of epilayer and substrate doping densities making it possible to provide epilayer properties such as doping densities, minority carrier diffusion length, and surface recombination velocity. © *2008 American Institute of Physics*. [DOI: 10.1063/1.2973461]

I. INTRODUCTION

Photoluminescence (PL) has been largely the domain of III-V semiconductor characterization in the past due to its high internal efficiency. Silicon, being an indirect band gap semiconductor, has low internal efficiency because most recombinations take place through Shockley–Read–Hall (SRH) or Auger recombination, neither of which emits light. In spite of the low internal efficiency, PL is now used to characterize Si, mainly through the introduction of the Silicon photoenhanced recombination (SiPHER) PL system, allowing nondestructive and contactless room-temperature wafer characterization. Light of 532 or 827 nm wavelength is the excitation source.[1] The high-intensity laser light, of 1 μm or 1 mm diameter, can map an entire wafer at modest resolution or scan a smaller area at higher resolution. The emitted light intensity depends on the defect and the doping densities, and hence can be used to map either one. PL has, of course, been used to characterize various aspects of Si and silicon-on-insulator for many years.[2] More recently, it has been used to characterize Si solar cell material and map iron densities in Si.[3]

To test our PL measurements, we first compared PL and surface photovoltage (SPV) (Ref. 4) measurements of one particular *p*-type Si bulk wafer shown in Fig. 1. SPV measures the minority carrier diffusion length L_n. All of the measurements in this paper are made at room temperature. The wafer was touched with a finger in region A, scratched with a metal pointer in region B, and subsequently annealed at 1100 °C for 2 min. Both figures clearly show the degradation in regions A and B. The metal scratches lead to significant PL and L_n reductions as expected. The finger-touched region A exhibits more SPV than PL degradation and shows a region beyond the original finger-touched area that affects the PL intensity. The higher resolution of the PL map is evident from these maps. From an analysis of the data, we conclude that the finger-touch contamination increases the surface and bulk recombination rates whereas in the metal-scratched region it is mainly the bulk recombination rate that is increased. These measurements established the usefulness of PL measurements for us.

Next we explored the possibility of PL characterization of epitaxial wafers. Here we report on results of PL measurements of n/n^+ epitaxial wafers. The PL data of such wafers are more difficult to analyze due to the different electrical and optical properties of the lightly doped epilayer and the more heavily doped substrate. Minority carrier lifetimes or diffusion lengths are difficult to determine in epitaxial layers, as the diffusion length is usually longer than the epilayer thickness and surface recombination, and epi/substrate interface recombination becomes quite important.

II. THEORY

We have developed one-, two-, and three-dimensional theories predicting the internal PL efficiency of bulk and epitaxial samples as a function of epilayer thickness (d_1), epi- and substrate doping densities (N_{D1} and N_{D2}), bulk trap density (N_T), photon flux density (Φ), and surface recombination velocity (s_r). The theory is verified by experimental data for bulk wafers. Here we apply it to epitaxial layers.

The sample in this paper is an *n*-type epitaxial layer on an n^+ substrate as shown in Fig. 2. Light of photon flux density Φ is incident on one side of the sample. For photon energies higher than the semiconductor band gap, each photon is assumed to generate one electron-hole pair. These excess carriers recombine. Some recombine radiatively while others recombine nonradiatively through SRH and Auger recombination. The time constants of these recombination events are the recombination lifetimes τ_{rad} and τ_{nonrad}. Some of the optically generated photons may be reabsorbed within the sample. This is typically a very small fraction in Si. Other photons are reflected back into the sample at the surface and others are emitted from the sample to be detected. The experimental data represent the external efficiency, i.e., photons out/photons in. The external PL efficiency is the internal efficiency times various geometric factors that depend on sample geometry and collection optics. Our theory determines the internal efficiency that we assume to be proportional to the external efficiency.

a)Electronic mail: dbaek1973@hotmail.com.

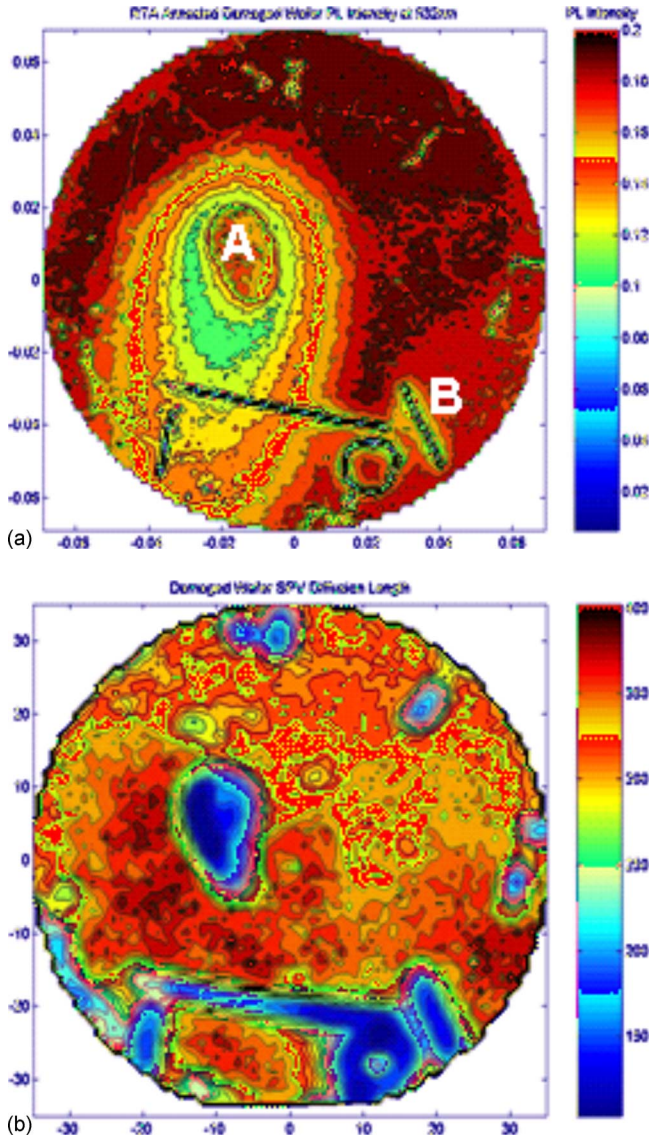

FIG. 1. (Color online) (a) PL and (b) SPV maps of a bulk Si wafer. Region A was touched with a finger and B was scratched with a metal pointer. The wafer was annealed at 1100 °C for 2 min, $\lambda = 532$ nm.

First we calculate the internal efficiency and compare it with experimental data for uniformly doped bulk Si wafers to verify our theory. The results are shown in Fig. 3. The normalized internal efficiency η exhibits a maximum at a doping density of around 3×10^{18} cm^{-3}. The efficiency depends on radiative and nonradiative recombinations. At low N_A, SRH recombination dominates and η is relatively independent of N_A. With increasing doping density τ_{rad} decreases $[\tau_{\text{rad}} = (BN_A)^{-1}]$, leading to an efficiency peak.[4] Subsequently, Auger recombination $[\tau_{\text{Auger}} = (CN_A^2)^{-1}]$ causes η to decrease at the higher N_A.[4]

The one-dimensional quantum efficiency equations are well known.[5] For the epitaxial sample, we solve the minority carrier continuity equation

$$D_p \nabla^2 \delta p(z) - \frac{\delta p(z)}{\tau_r} = -\alpha \phi (1-R) e^{-\alpha z},$$

subject to the boundary conditions

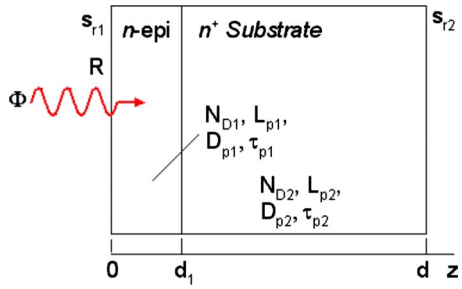

FIG. 2. (Color online) Epitaxial sample configuration.

$$\delta p_1(0) = \frac{D_{p1}}{s_{r1}} \cdot \left. \frac{\partial \delta p(z)}{\partial z} \right|_{z=0}, \quad \delta p_1(d_1) = \delta p_2(d_1),$$

$$\delta p_2(d) = -\frac{D_{p2}}{s_{r2}} \cdot \left. \frac{\partial \delta p(z)}{\partial z} \right|_{z=d}, \quad D_{p1} \left. \frac{\partial \delta p_1(z)}{\delta z} \right|_{z=d_1} = D_{p2} \left. \frac{\partial \delta p_2(z)}{\delta z} \right|_{z=d_1}.$$

The internal PL efficiency is given by[6]

$$\eta_{\text{int}} = \int_0^d \frac{\delta p}{\tau_{\text{rad}}} \exp(-\beta x) dx \approx \int_0^d \frac{\delta p}{\tau_{\text{rad}}} dx,$$

where d is the sample thickness, δn is the excess minority carrier density, and β is the absorption coefficient of the *generated* light within the sample. Since the emitted light in Si has a wavelength near the band gap, the absorption coefficient β is very low, ≈ 2 cm^{-1} for $h\nu = 1.12$ eV, and $\exp(-\beta x)$ is neglected.

The calculated excess carrier densities for n/n^+ epitaxial samples are shown in Fig. 4. We use the absorption coefficients $\alpha = 9100$ cm^{-1} for $\lambda = 532$ nm and $\alpha = 675$ cm^{-1} for $\lambda = 827$ nm.[7] Photon flux densities in the SiPHER tool are in the range of 10^{21}–10^{22} cm^{-2} s^{-1}, leading to high excess carrier densities. For the 532 nm wavelength excitation light, the optical absorption depth is around 10^{-4} cm. Figure 4 shows the excess carrier densities to be reasonably constant over the epilayer thickness, but drop significantly in the substrate because the lifetime in the substrate is lower than in the epilayer due to Auger recombination. This figure shows

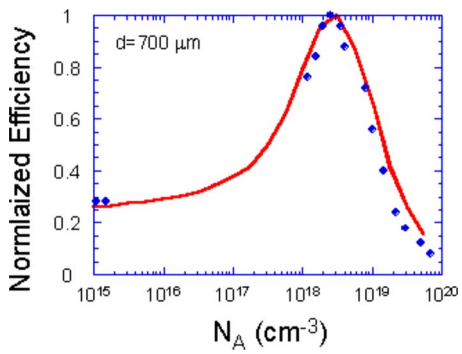

FIG. 3. (Color online) Normalized efficiency vs doping density. Calculated for $\sigma_n = \sigma_p = 10^{-15}$ cm^2, $\lambda = 827$ nm, $s_{r1} = 5000$ cm/s, $s_{r2} = 1000$ cm/s, $N_T = 2 \times 10^{11}$ cm^{-3}, $\Phi = 5 \times 10^{21}$ photons/cm^2 s, and $d = 700$ μm. Data courtesy of A. Buczkowski, SUMCO.

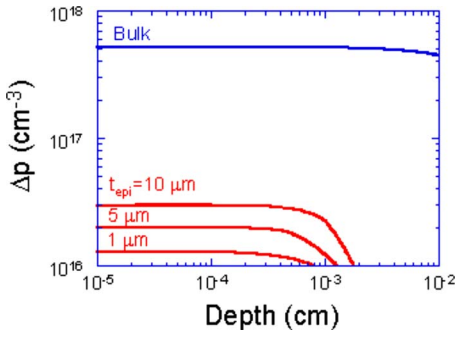

FIG. 4. (Color online) Excess carrier density vs sample depth as a function of epilayer thickness. Also shown is the excess carrier density for a bulk Si wafer. $N_{epi}=10^{15}$ cm^{-3}, $N_{sub}=10^{19}$ cm^{-3}, $N_{bulk}=10^{15}$ cm^{-3}, $N_T=10^{11}$ cm^{-3}, $s_{r1}=1000$ cm/s, $s_{r2}=5000$ cm/s, $\lambda=532$ nm, and $\Phi=10^{21}$ photons/s cm^2.

excess carriers diffuse into the substrate even though the n/n^+ interface is a minority carrier reflecting surface. We also show the excess carrier density for a lightly doped bulk Si wafer for comparison. Δp for the bulk wafer is significantly higher than the epiwafer because the nonradiative lifetime of the bulk wafer is higher.

To determine the PL response as a function of epilayer thickness, we angle lapped a 50 μm thick epitaxial layer as shown in Fig. 5. This gives us varying epilayer thicknesses in one sample with uniform parameters (N_D, N_T, etc.). Using several nonangle lapped samples with varying epilayer thicknesses runs the risk of varying doping and trap densities among the samples. The PL light beam was swept along the beveled surface and the experimental PL intensity data are shown in Fig. 6. The "0" and "50" on the depth scale in Fig. 6 are indicated in Fig. 5.

The PL intensity for the 827 nm light gradually increases toward the substrate but the intensity for the 532 nm light remains reasonably constant to 30 μm and then increases rapidly as the incident light approaches the substrate. Because 827 nm photons penetrate ten times deeper than 532 nm photons, the PL intensity for 827 nm is affected by both epilayer and bulk properties. The bulk PL intensity is higher than the epilayer PL intensity because SRH recombination dominates and η is relatively independent of the doping density in the epilayer, but radiative recombination dominates in the bulk and the efficiency increases, as shown in Fig. 3.

III. EPITAXIAL WAFER LIFETIME MODELING AND CHARACTERIZATION

We presented the PL efficiency theory and correlated it with PL intensity measurements for different doping densities earlier[8] and now apply that theory to epilayer characterization as illustrated in Fig. 7. First, the beveled epiwafer is

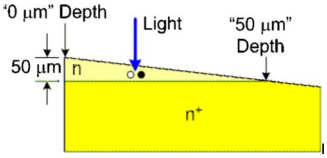

FIG. 5. (Color online) Substrate: $N_D=6\times10^{17}$ cm^{-3}, Sb-doped; epitaxial layer: $N_D=1.6\times10^{14}$ cm^{-3}, P-doped. Wafer beveled at 3°, dipped in HF, exposed to air for a few hours, and then measured.

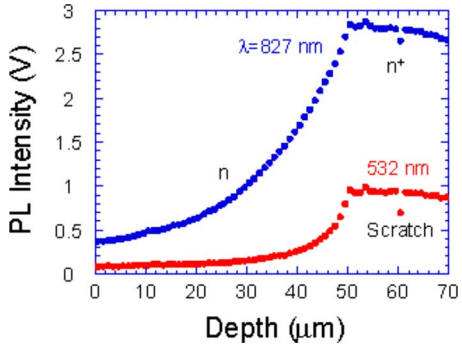

FIG. 6. (Color online) PL intensity data for the epi sample in Fig. 5.

measured with $\lambda=532$ and 827 nm incident light. We define the PL *intensity ratio* as $R_{PL}=I_{PL}(827)/I_{PL}(532)$ and the PL *efficiency ratio* as R_{PLE}. Here, I_{PL} is the PL measured intensity. We determine the PL intensity ratio R_{PL} at the epiwafer top through the epilayer and the substrate. The PL intensity at the top contains mostly epilayer properties and the PL intensity for the substrate contains only bulk properties. The two PL intensity ratios yield the surface recombination velocity s_r by the PL intensity ratio method.[8] Based on s_r and the doping concentration, we compute the PL efficiency to obtain two values of the PL efficiency ratio R_{PLE} for the epilayer and the substrate. When R_{PL} matches R_{PLE}, we obtain the PL intensity profile of the epiwafer for $\lambda=532$ and 827 nm. For the next step, we use a curve fitting method because the PL efficiency profile is calculated as a function of doping concentration as shown in Fig. 8(a), but the PL intensity is measured as a function of depth as shown in Fig. 8(b).

We measured the PL intensity for a 5° beveled 61 μm thick epiwafer, doped at 2×10^{14} cm^{-3} on a substrate doped at 10^{19} cm^{-3} as shown in Fig. 8(b). The PL intensity for the 532 nm wavelength varies little up to 40 μm and then increases to 55 μm, which is the interface between the epilayer and the substrate. Subsequently the PL intensity somewhat decreases and remains constant upon reaching the substrate. We explain this behavior using the PL efficiency versus doping concentration profile graphs in Fig. 8(a). The PL efficiency is mainly constant until the doping concentration reaches 10^{17} cm^{-3}, increases to 10^{18} cm^{-3}, and then de-

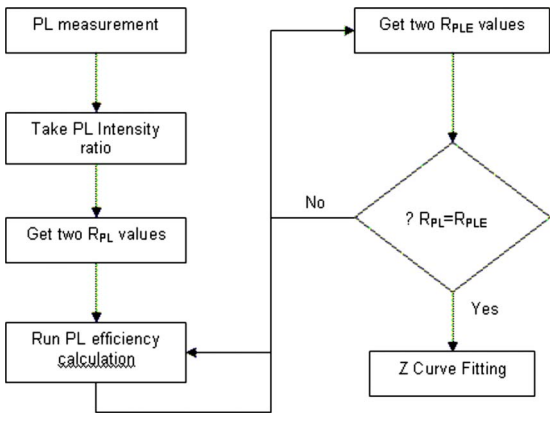

FIG. 7. (Color online) Epiwafer PL intensity fitting method.

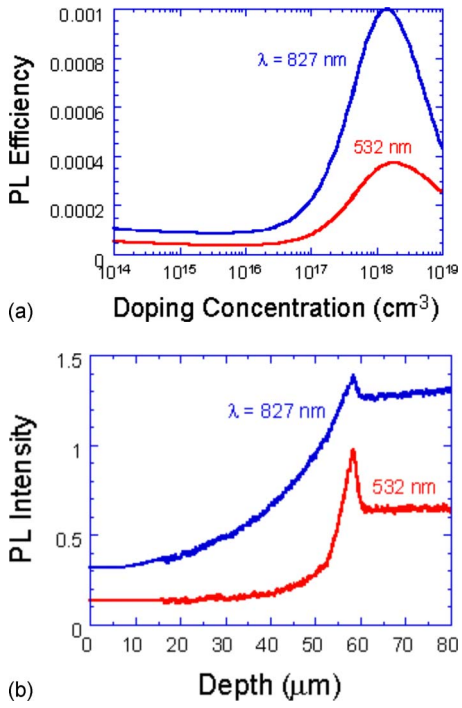

FIG. 8. (Color online) (a) Calculated PL efficiency and (b) beveled epiwafer PL intensity profile for λ=532 and 827 nm.

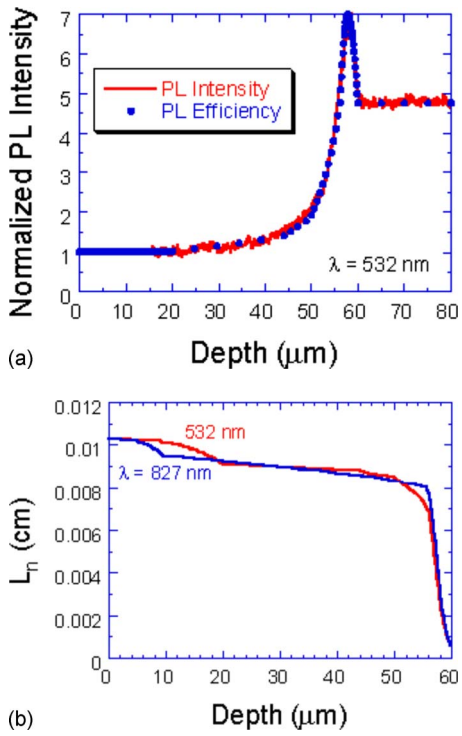

FIG. 9. (Color online) (a) PL intensity vs depth profile by the depth vs doping concentration fitting method. (b) Minority carrier diffusion length vs depth profile by PL efficiency calculation.

creases because radiative recombination dominates between 10^{17} and 10^{18} cm^{-3}. Beyond that, the higher doping concentration-dependent Auger recombination takes over. As the thickness decreases, the epilayer doping concentration plays only a minor role in the PL intensity. The effective doping concentration, defined as a combination of epilayer doping concentration and bulk doping concentration, is higher for thinner epilayers; the PL intensity increases, then the bulk doping concentration dominates and the PL intensity decreases.

From the PL intensity fitting method, we obtain PL intensity data from the measurement as shown in Fig. 8(b). Then we obtain initial parameters such as surface recombination velocity, which is 30 000 cm/s in this sample, from the PL intensity ratio method.[8] Now, we calculate the PL efficiency as a function of doping concentration as shown in Fig. 8(a). Based on Figs. 8(a) and 8(b), if we take the normalized data then fit the PL intensity and PL efficiency from the doping concentration to the depth profile, we obtain the PL intensity versus depth profile in Fig. 9(a).

Based on the fitting method, we determine the minority carrier diffusion length from the PL efficiency calculations as shown in Fig. 9(b). The diffusion length of the epilayer is about 100 μm for both 532 and 827 nm. For thinner epilayers, the diffusion length is lower and decreases sharply at the epilayer/substrate interface. Figure 9(b) shows two slightly different diffusion length profiles for λ=532 and 827 nm. For the longer wavelengths, the penetration depth is higher, e.g., 10 μm penetration depth for 827 nm and 1 μm for 532 nm. The epilayer diffusion length is initially the same for the two wavelengths, then diverges slightly at around z =10 μm due to deeper penetration of the 827 nm wavelength.

As the 827 photons penetrate deeper than the 532 nm photons, the peak of the excess carrier generation is different when the excess carriers diffuse toward the substrate. The excess carriers for 827 nm are close to the substrate, leading to a higher recombination rate than for 532 nm, and the diffusion length for 827 nm is shorter than for 532 nm, even though the doping concentration is the same. Hence, the effective doping concentration for 827 nm is higher than for 532 nm or the diffusion length is shorter at the same position. Beyond z=20 μm, the diffusion lengths are similar for both 532 and 827 nm. In this profile, we are able to obtain the effective diffusion lengths of the epilayer. In this sample the epilayer thickness is 61 μm and the epilayer diffusion length is about 100 μm. For a 30 μm thick epilayer, the effective diffusion length is about 90 μm. The substrate diffusion length is about 11 μm.

IV. SUMMARY

Room-temperature band-edge PL metrology is used for contamination and defect characterization of Si and related materials. We have shown previously how to extract surface recombination velocity from such measurements. Here we show the application of room-temperature PL measurements to characterize silicon epitaxial layers. We show PL to be a powerful characterization technique providing information about doping concentration, diffusion length, and surface recombination velocity. We have developed the relevant theory to explain both bulk and epitaxial sample behaviors and extract the minority carrier diffusion length.

ACKNOWLEDGMENTS

The research leading to this paper was partially funded by the Silicon Wafer Engineering and Defect Science (SiWEDS) Consortium (Hynix Semiconductor., Intel Corp., LG Siltron Inc., MEMC, Samsung Electronics Co., Siltronic, SOITEC, and Sumco TECHXIV).

[1]A. Buczkowski, in *Analytical and Diagnostic Techniques for Semiconductor Materials, Devices, and Processes VII*, edited by D. K. Schroder, L. Fabry, R. Hockett, H. Shimizu, and A. Diebold (Electrochemical Society, Pennington, NJ, 2007), Vol. 11, pp. 109–122.
[2]M. Tajima, Appl. Phys. Lett. **32**, 719 (1978); M. Tajima, T. Masui, T. Abe, and T. Iizuka, in *Semiconductor Silicon/1981*, edited by H. R. Huff, R. J. Kriegler, and Y. Takeishi (Electrochemical Society, Pennington, NJ, 1981), pp. 72–89; M. Tajima, Jpn. J. Appl. Phys., Part 2 **21**, L227 (1982); M. Tajima, S. Ibuka, H. Aga, and T. Abe, Appl. Phys. Lett. **70**, 231 (1997); M. Tajima, H. Yoshida, S. Ikuba, and S. Kishino, Jpn. J. Appl. Phys., Part 2 **42**, L429 (2003).
[3]D. Macdonald, J. Tan, and T. Trupke, J. Appl. Phys. **103**, 073710 (2008).
[4]D. K. Schroder, *Semiconductor Material and Device Characterization* (Wiley, New York, 2006), Chap. 7.
[5]G. Duggan and G. B. Scott, J. Appl. Phys. **52**, 407 (1981).
[6]E. W. Williams and R. A. Chapman, J. Appl. Phys. **38**, 2547 (1967).
[7]M. A. Green, *High Efficiency Silicon Solar Cells* (Trans Tech, Zürich, 1987), pp. 228–230.
[8]D. Baek, S. Rouvimov, B. Kim, T.-C. Jo, and D. K. Schroder, Appl. Phys. Lett. **86**, 112110 (2005).